Available online at https://link.springer.com/journal/42241
http://www.jhydrodynamics.com
**Journal of Hydrodynamics**, 2023, 35(4): 803-810
https://doi.org/10.1007/s42241-023-0059-2

# Scaling laws for the intermittent swimming performance of a flexible plate at low Reynolds number

Lin-lin Kang[1], Shi-xian Gong[1], Xi-Yun Lu[2], Wei-cheng Cui[1], Di-xia Fan[1*]
1. *Key Laboratory of Coastal Environment and Resources of Zhejiang Province, School of Engineering, Westlake University, Hangzhou 310030, China*
2. *Department of Modern Mechanics, University of Science and Technology of China, Hefei 230026, China*

(Received January 14, 2023, Revised July 18, 2023, Accepted July 26, 2023, Published online October 20, 2023)


**Abstract:** Many species of fish and birds travel in intermittent style, yet the combined influence of intermittency and other body kinematics on the hydrodynamics of a self-propelled swimmer is not fully understood. By formulating a reduced-order dynamical model for intermittent swimming, we uncover scaling laws that link the propulsive performance (cursing Reynolds number $Re_c$, thrust $\overline{T}$, input power $\overline{P}$ and cost of transport $COT$ to body kinematics (duty cycle $DC$, flapping Reynolds number $Re_f$). By comparing the derived scaling laws with the data from several previous studies and our numerical simulation, we demonstrate the validity of the theory. In addition, we found that $Re_c$, $\overline{T}$, $\overline{P}$ and $COT$ all increase with the increase of $DC$, $Re_f$. The model also reveals that the intermittent swimming may not be inherently more energy efficient than continuous swimming, depending on the ratio of drag coefficients between active bursting and coasting.

**Key words:** Propulsion, intermittent swimming, scaling law

## 0. Introduction

Known as burst and coast, the intermittent dynamics are exploited across fish species[1-4] with the behavioral context of preying, mating, habitat assessment, and general travel[5]. From a hydrodynamic point of view, individual fish is supposed to spend less energy and travel a longer distance by alternating between active swimming and gliding.

Compared with continuous swimming (CS), hydrodynamics of fish's intermittent swimming (IS) is yet to be thoroughly studied. However, results of the biological studies on IS[6-7] have shown a decrease in the locomotion cost of fish. The fluid analysis has attributed such an increase in energy efficiency to the viscous Bone-Lighthill boundary layer thinning mechanism[6] and inviscid Garrick mechanism[8], which inspired a series of subsequent studies on optimal IS gaits of plates/foils with prescribed or self-propelled trajectories[9-13].

The aforementioned studies explored the effect of different parameters on the energy efficiency of IS versus CS, including duty cycles, cruising Reynolds number[9], reduced frequency[8], bending stiffness[12] and fish locomotion type[14]. These results demonstrated that the energy efficiency of IS may not be inherently higher than CS and is highly dependent on the selection of the parameters, which clearly illustrates the complexity of the problem and calls for a fluid scaling law to uncover the relationship between the kinematics and dynamics of IS.

Starting from Theodorsen's conclusion[15] on the power of an oscillating foil that scales as $P \sim St^2$ for small amplitude and $P \sim St^3$ for large amplitude, where $St$ is the Strouhal number, the study of scaling laws has always been one of the key research areas in the field of bio-inspired propulsion. In particular, by focusing on the rigid forced oscillating foils in a free stream[16-18], researchers observed the coherent reverse Karman vortex street behind a flapping foil with optimal efficiency in the range of $St \sim 0.25\text{-}0.35$ and with a thrust scaling as $T \sim (fA_t)^2$ ($A_t$ is the flapping amplitude of the trailing

Project supported by the National Key Research and Development Program of China (Grant No. 2022YFC2805200), the National Natural Science Foundation of China (Grant No. 12102365).
**Biography:** Lin-lin Kang (1991-), Female, Ph. D.,
E-mail: kanglinlin@westlake.edu.cn
**Corresponding author:** Di-xia Fan,
E-mail: fandixia@westlake.edu.cn

edge), which coincides with the dynamics of the swimming animals[19]. Furthermore, by studying the unconstrained foil/self-propelled flexible plate in the still water, results[20-21] indicated that the thrust $T \sim (fA_t)^{2.5}$ and drag $D \sim U^{4/3}$ may scale differently compared with those of rigid forced oscillating foils in a free stream.

It is important to note that most of the previous works on the bio-propulsion scaling law are based on the CS assumption[22]. Several recent works on the IS[10, 19, 23] indicated that the intermittent dynamics does not follow the scaling law derived for the CS behavior, and additional effects must be considered[8]. Therefore, we aim to establish the scaling law for IS of a self-propelled flexible body by examining the effect of different IS parameters on swimming performance. To realize it, we simulate the IS of a self-propelled flexible plate to validate the scaling law derived from a simplified dynamical IS model. In addition, we investigate the effect of body kinematics, i.e., duty cycle, flapping frequency, heaving amplitude, and pitching amplitude on IS.

## 1. Physical model and numerical methods

We consider the IS of a self-propelled flexible plate forced to pitch $(\theta)$ or heave $(h)$ in a multiple tail-beat (MT) mode[24], while swimming freely in the $x$ direction (Figs. 1(a), 1(b)). The prescribed motions of $\theta(t)$, $h(t)$ are given in Eqs. (1), (2) (Fig. 1(c)).

$$\theta(t) = \theta_0 \sin(2\pi f_b t), \quad 0 < t \le T_b \tag{1a}$$

$$\theta(t) = 0, T_b < t \le T_{cyc} \tag{1b}$$

$$h(t) = A\cos(2\pi f_b t), \quad 0 < t \le T_b \tag{2a}$$

$$h(t) = A, \quad T_b < t \le T_{cyc} \tag{2b}$$

where $\theta_0$ and $A$ are the pitching and heaving amplitudes. $T_{cyc}$ is the full burst and coast cycle time consisting of a burst phase $(T_b)$. The duty cycle $DC$ is defined as $DC = T_b / T_{cyc}$, reflecting the intermittency of the motion.

The motions of the fluid and the elastic plate are governed by the incompressible continuity equation and Navier-Stokes equations, Eq. (3), and the nonlinear partial differential equations, Eq. (4):

$$\nabla \cdot \boldsymbol{u} = 0, \quad \frac{\partial \boldsymbol{u}}{\partial t} + \boldsymbol{u} \cdot \nabla \boldsymbol{u} = -\frac{1}{\rho}\nabla p + \frac{\mu}{\rho}\nabla^2 \boldsymbol{u} + \boldsymbol{f} \tag{3}$$

$$\rho_s h \frac{\partial^2 \boldsymbol{X}}{\partial t^2} - \frac{\partial}{\partial s}\left[ Eh\left(1 - \left|\frac{\partial \boldsymbol{X}}{\partial s}\right|^{-1}\right)\frac{\partial \boldsymbol{X}}{\partial s}\right] + EI\frac{\partial^4 \boldsymbol{X}}{\partial s^4} = \boldsymbol{F}_s \tag{4}$$

where $\rho$, $\mu$, $\boldsymbol{u}$ and $p$ are the fluid density, dynamic viscosity, velocity and pressure, $s$ and $\boldsymbol{X}$ are the Lagrangian coordinate and the position vector of the plate, $\rho_s h$, $Eh$ and $EI$ describe the plate linear mass density, the stretching and bending rigidity, $\boldsymbol{f}$ and $\boldsymbol{F}_s$ are the Eulerian and Lagrangian forces between the fluid and the plate. The boundary conditions are identical to those described by Liu et al.[21].

In our simulation, $\rho$, $\mu$, $L$ and the reference velocity $U_{ref}$ are fixed. The governing equations hence are normalized by $\rho$, $L$ and $U_{ref}$ with the characteristic time as $T_{ref} = L / U_{ref}$, which results in four key dimensionless parameters $Re = \rho U_{ref} L / \mu$, $M = \rho_s h / \rho L$, $S = Eh / (\rho U_{ref}^2 L)$ and $K = EI / (\rho U_{ref}^2 L^3)$ as the Reynolds number, the plate mass ratio, stretching and bending stiffness.

Equtions (3), (4) are solved by the lattice Boltzmann method[25] and a nonlinear finite element method[26], and the immersed boundary method is used to treat the fluid-plate interaction[27], see previous papers[11, 27] for detailed description of the numerical

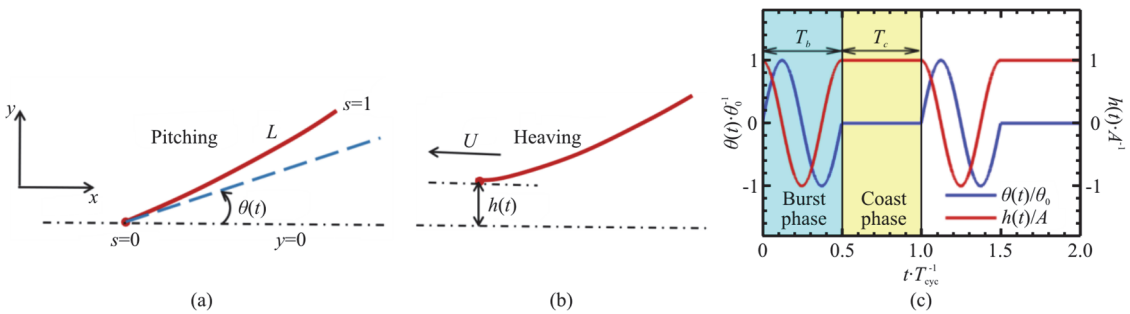


Fig. 1 (Color online) Sketch of the (a) pitching and (b) heaving flexible plates ($L$ is the length of the plate, $U$ is the horizontal velocity of the leading edge of the plate). (c) Intermittent functions of pitching and heaving motion

method. The computational fluid domain is $[-15,25]$ in the $x$ direction and $[-15,15]$ in the $y$ direction. It is large enough to eliminate the blocking effects of the outer boundaries. The mesh is uniform in the $x$ and $y$ directions with spacing $\Delta x=\Delta y=0.01L$. The time step for the simulations of fluid motion and plate deformation is $\Delta t=T_b/10\,000$.

In order to validate the numerical methods, a self-propelled flexible plate heaving intermittently in MT mode[12] was considered with $Re=200/\pi$, $A=0.5$, $M=0.2$, $K=\pi^2$, $S=1\,000\pi^2$, $DC=0.5$. It should be noted that the characteristic velocities are $U_{\text{ref}}=Lf_b$ and $2\pi Af$ in the present study and in Liu et al.[12]. Figure 2(a) shows the horizontal velocity of the leading edge of plate. It can be seen that the present result is in good agreement with the previous study[12]. Moreover, the flexible plate pitching intermittently in MT mode with $Re=200$, $A=0.5$, $M=0.2$, $K=10$, $S=1\,000$ and $DC=0.5$ was also considered to study the grid independence and time-step independence. It is seen in Fig. 2(b) that, $\Delta x=0.01L$, $\Delta t=0.0001T_b$ are sufficient to achieve accurate simulation results.

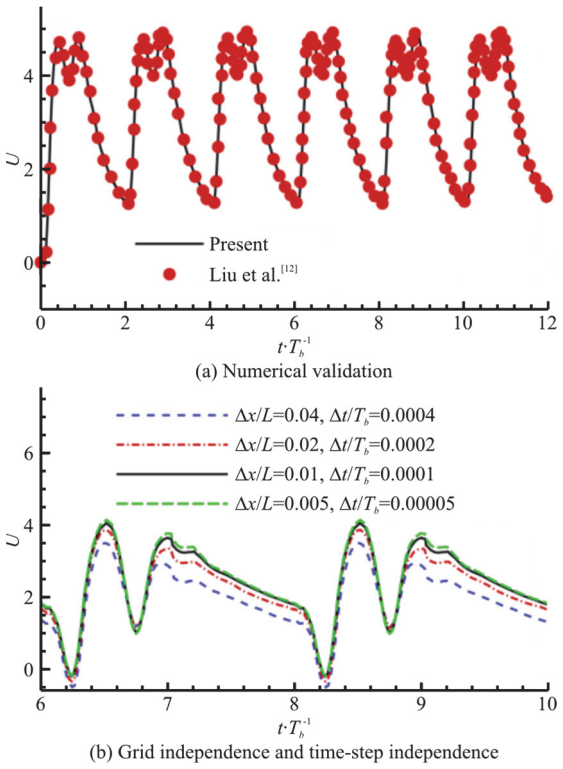


(a) Numerical validation

(b) Grid independence and time-step independence

Fig. 2 (Color online) The horizontal velocity of the leading edge of plate as a function of time

## 2. Results and discussion

In our simulation, we set $Re=200$, $M=0.2$ and $S=1\,000$ which is large enough so that the plate can be considered as inextensible. We study the IS hydrodynamics over a large range of $A/L\in[0.1,\,0.5]$, $\theta_0\in[\pi/18,\pi/6]$, $K\in[10,100]$, $DC\in[0.25,1]$ and the non-dimensional flapping frequency $f=f_b/f_b^*\in[0.5,2]$. It is noted that for real fish, $K\sim O(10)$, for example, $K\approx 25\text{-}230$ for the tail-fin of a gold fish (Carassius auratus), corresponding to the large forward speeds and high propulsive efficiencies[28].

### 2.1 *Propulsive performance*

First, the propulsive performance (the velocity $U$, force on the plate $\boldsymbol{F}_s$ and input power $P$ at each instant) of a self-propelled plate in a full burst and coast cycle is shown in Fig. 3. It is noted that $\boldsymbol{F}_s=\boldsymbol{F}^n+\boldsymbol{F}^\tau$, where $\boldsymbol{F}^n$ is the pressure-dominated normal force, $\boldsymbol{F}^\tau$ is the tangential force as a result of the viscous effects.

$$\boldsymbol{F}^n=F_x^n\boldsymbol{e}_x+F_y^n\boldsymbol{e}_y,\quad \boldsymbol{F}^\tau=F_x^\tau\boldsymbol{e}_x+F_y^\tau\boldsymbol{e}_y \tag{5}$$

It is seen that $U$ oscillates in the burst phase and decreases monotonically in the coast phase (Fig. 3(a)), as the energy input mainly occurs in the burst phase (Fig. 3(c)). Figure 3(b) shows that in the coast phase, for both heaving and pitching, the drag is mainly provided by $\boldsymbol{F}^\tau$, while little thrust can be obtained due to no active flapping. In the burst phase, $\boldsymbol{F}^\tau$ and $\boldsymbol{F}^n$ may both contribute significantly to either thrust and drag for a pitching plate, while for a heaving plate, the drag and thrust are more strongly correlated to $\boldsymbol{F}^\tau$ and $\boldsymbol{F}^n$ separately. In the following study, we define the thrust $T$ and drag $D$ on the plate same as in Bottom et al.[29].

$$-T(t)=\frac{1}{2}\left(F_x^n-\left|F_x^n\right|\right)+\frac{1}{2}\left(F_x^\tau-\left|F_x^\tau\right|\right),$$

$$D(t)=\frac{1}{2}\left(F_x^n+\left|F_x^n\right|\right)+\frac{1}{2}\left(F_x^\tau+\left|F_x^\tau\right|\right) \tag{6}$$

Next, we focus on the time-averaged cruising speed $U_c$, thrust $\overline{T}$, power consumption $\overline{P}$ and the cost of transport $COT$ of the entire burst and coast period (Fig. 4). Specifically, the cost of transport is the energy required to transport a unit mass over a unit distance, which can be calculated as $COT=\overline{P}/mU_c$. In Fig. 4, except for several data points of large duty cycles $(DC>0.75)$, $U_c$, $\overline{T}$, $\overline{P}$ and $COT$ all

increase with increasing $DC$, $\theta_0$, $A$ and $f$. Namely, a stronger active motion in the burst phase will result in larger thrust, faster speed, higher power consumption and larger cost of transport.

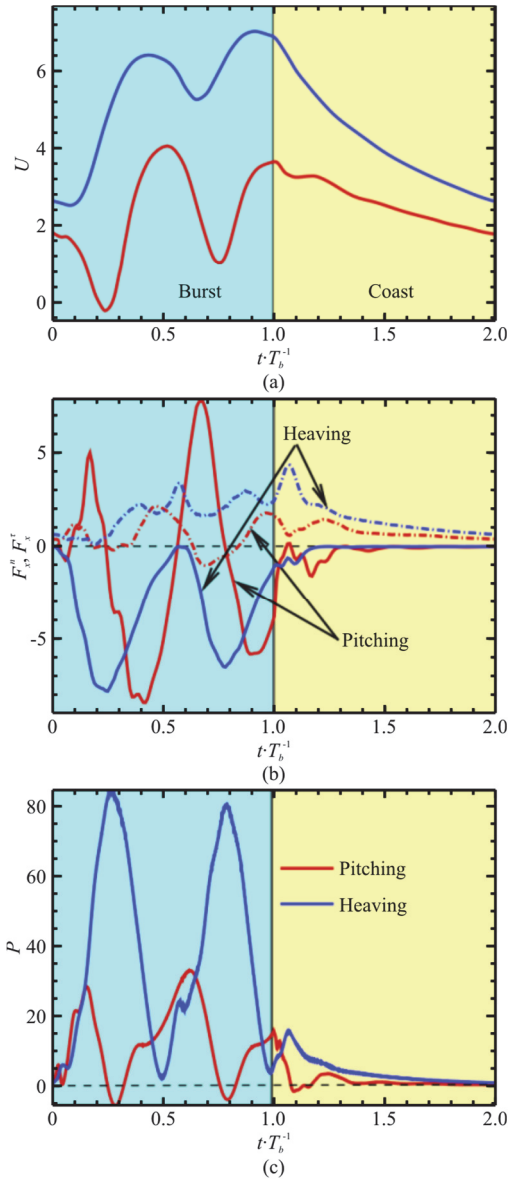


Fig. 3 (Color online) (a) $U$ (b) $\boldsymbol{F}^n$, $\boldsymbol{F}^\tau$, (c) $P$ for pitching ($\theta_0 = \pi/6$, $K = 10$, $f = 1$, $DC = 0.5$) and heaving ($A = 0.5$, $K = 10$, $f = 1$, $DC = 0.5$) plates as functions of time in a cycle period. Solid and dashed lines in subfigure (b) represent $F_x^n$, $F_x^\tau$

## 2.2 *Dynamical model for intermittent swimming*

To interpret the above findings, we formulate a simplified dynamical model for the IS of a plate freely moving horizontally while flapping vertically (Fig. 1). We assume that the thrust only occurs in the burst phase, while the drag applies in the entire cycle (Fig. 3(b))[7].

$$m\dot{u} = T - D_b, \quad 0 < t \le T \tag{7a}$$

$$m\dot{u} = -D_c, \quad T_b < t \le T_{\text{cyc}} \tag{7b}$$

where $m$ is the mass of the plate, $u$ is the horizontal velocity, $D_b$ and $D_c$ are the drags on the plate during burst and coast phases.

The model assumes that the thrust scales with the square of the plate's flapping velocity $v$ [6, 10, 19, 29], i.e.

$$T = cv^2 \tag{8}$$

where $c$ is the constant coefficient, $c_t$ is the thrust coefficient of the plate. The drag scales with $u$ [19, 29], i.e.

$$D_c = \mathrm{d}u^\alpha, \quad D_b = \beta \mathrm{d}u^\alpha \tag{9}$$

where $d$ is the constant coefficient, $c_d$ is the drag coefficient of the plate in coast phase[6]. Usually, $\alpha = 3/2$ for laminar flow, $\alpha = 2$ for turbulent flow[19]. $\beta$ is the ratio of drag coefficient between active bursting and coasting, which is usually greater than 1. The previous experimental data[6, 30] suggest that the drag of fish when swimming is increased over the value for a rigid body by a factor of approximately 3. Substituting Eqs. (8), (9) into Eq. (7), and integrating Eq. (7) in the burst and coast periods, we can obtain

$$m(U_f - U_i) = \int_0^{T_b} (cv^2 - \beta \mathrm{d}u^\alpha)\,\mathrm{d}t,$$

$$m(U_i - U_f) = \int_{T_b}^{T_{\text{cyc}}} (-\mathrm{d}u^\alpha)\,\mathrm{d}t \tag{10}$$

where $U_i$ and $U_f$ denote the initial and final horizontal velocities of the burst phase. Adding the two equations in Eq. (10) yields

$$\int_0^{T_b} cv^2 \mathrm{d}t = \int_0^{T_b} \beta \mathrm{d}u^\alpha \mathrm{d}t + \int_{T_b}^{T_{\text{cyc}}} \mathrm{d}u^\alpha \mathrm{d}t \tag{11}$$

Assuming that $u(t)$ is a linear function of time in both burst and coast phases, the momentum of drag in a cycle is

$$I_d = (\beta - 1 + DC^{-1})\,\mathrm{d}T_b U_c^\alpha \left[1 + O\left(\frac{\Delta^2}{U_c^2}\right)\right]$$

where $U_c = 1/2(U_f + U_i)$, $\Delta = 1/2(U_f - U_i)$.

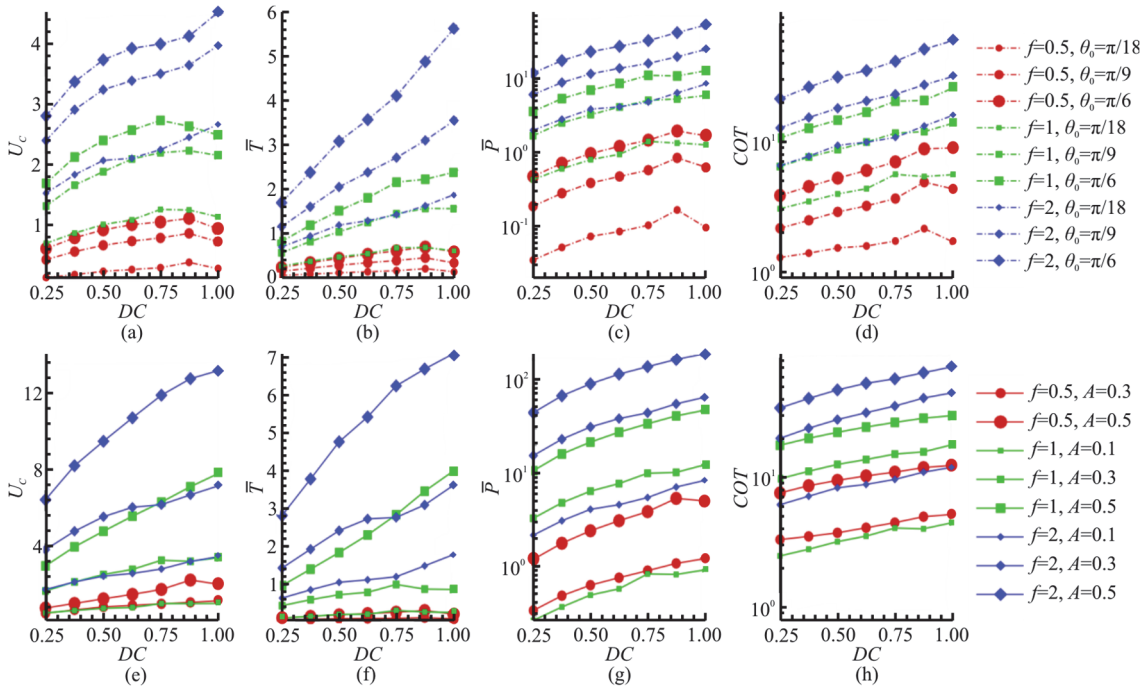


Fig. 4 (Color online) (a) $U_c$, (b) $\overline{T}$, (c) $\overline{P}$ and (d) $COT$ as functions of $DC$ for pitching plates with various $\theta_0$, $f$ at fixed $K=10$. Panels (e)-(h) are the corresponding results for heaving plates

Taking the intermittent heaving motion, Eq. (2), for an example, the momentum of thrust in a cycle is $I_t = 2c(\pi A f_b)^2 T_b$. Usually, $\Delta^2 / U_c^2 \ll 1$, thus by ignoring the second-order smaller term, Eq. (11) can be reduced to

$$\frac{c}{2d}(2\pi A f_b)^2 = (\beta - 1 + DC^{-1})U_c^{\alpha} \tag{12}$$

Replacing the above equation by dimensionless parameters, i.e., the flapping Reynolds number $Re_f = 2\rho f_b AL/\mu$ ($Re_f = 2\rho f_b L^2\theta_0/\mu$ for pitching motion), the cruising Reynolds number $Re_c = \rho U_c L/\mu$, we can obtain

$$Re_c^{\alpha} \sim \frac{Re_f^2}{\beta - 1 + DC^{-1}} \tag{13}$$

The average thrust in the burst phase $\overline{T}_b$ and the average drag in one cycle $\overline{D}$ are scaled as

$$\overline{T}_b = \frac{\overline{T}}{DC} = \frac{1}{T_b}\int_0^{T_b} cv^2 \mathrm{d}t \sim Re_f^2 \tag{14}$$

$$\overline{D} = \frac{1}{T_{cyc}}\left(\int_0^{T_b} \beta \mathrm{d}u^{\alpha}\mathrm{d}t + \int_{T_b}^{T_{cyc}} \mathrm{d}u^{\alpha}\mathrm{d}t\right) \sim [(\beta - 1)DC + 1]Re_c^{\alpha} \tag{15}$$

Following the elongated-body theory[6], it is easy to derive that the average input power in the burst phase $\overline{P}_b$ satisfies

$$\overline{P}_b = \frac{\overline{P}}{DC} \sim Re_f^3 \tag{16}$$

Based on Eqs. (13), (16), $COT = \overline{P}/mU_c$ is scaled as

$$COT \sim Re_f^{(3-2/\alpha)}[DC(\beta - 1 + DC^{-1})^{1/\alpha}] \tag{17}$$

By the scaling laws derived above, we demonstrate the positive correlation between $(U_c, \overline{T}, \overline{P}, COT)$ and $(\theta_0, A, f, DC)$ clearly shown in Fig. 4. Furthermore, by replacing $Re_f$ with $Re_c$ in Eq. (17), we derive the relation between $Re_c$ and $COT$ as

$$COT \sim Re_c^{(1.5\alpha - 1)}[DC(\beta - 1 + DC^{-1})^{1.5}] \tag{18}$$

Interestingly, we notice that at a given $Re_c$, for the model of same length $L$ swimming at same $U_c$, the minimum of $COT$ is achieved for the most efficient duty cycle of $DC_{ME} = [2(\beta - 1)]^{-1}$ ($\partial COT/\partial DC = 0$, $\partial^2 COT/\partial DC^2 > 0$). Since $DC \in$

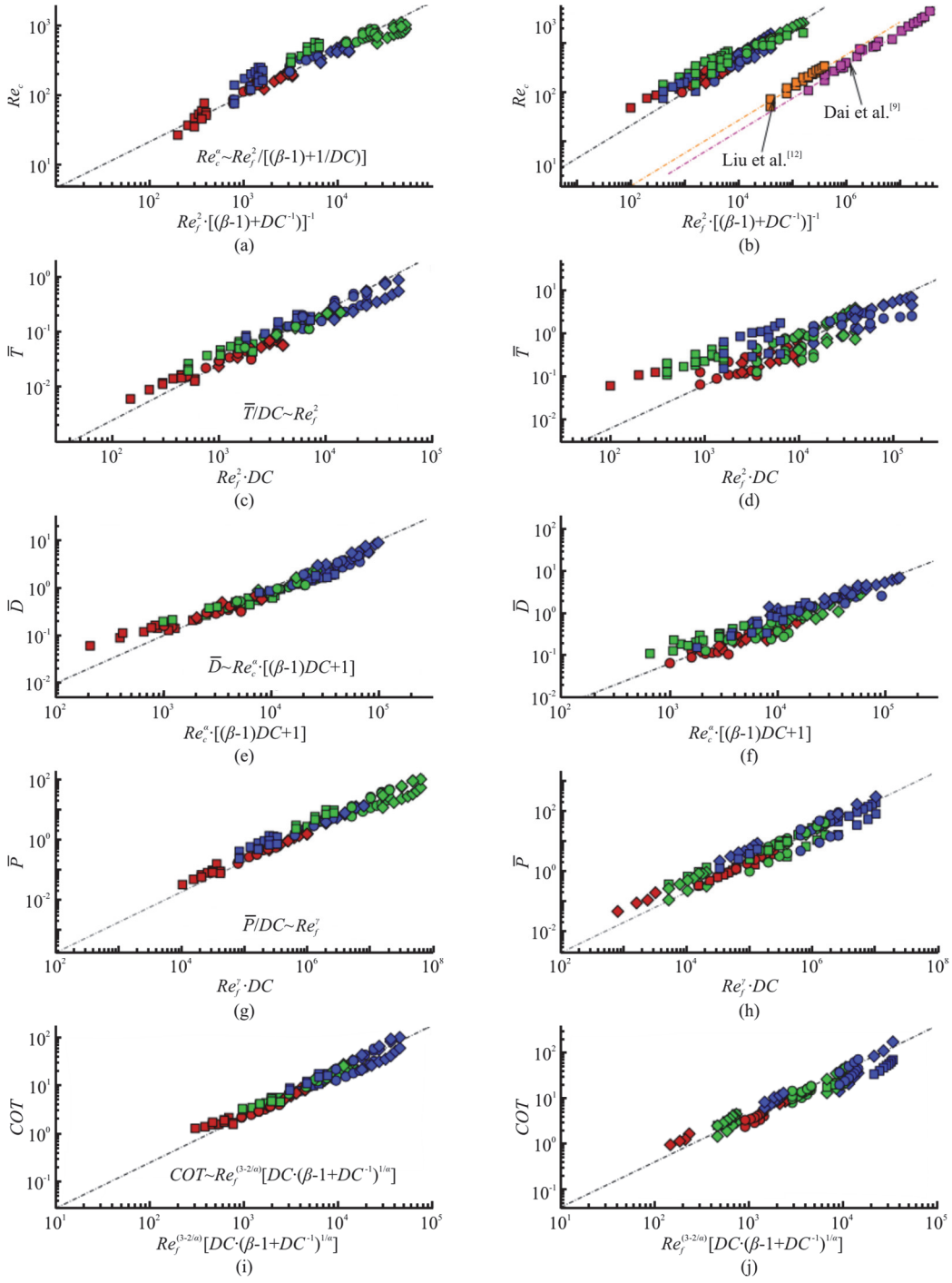


Fig. 5 (Color online) $Re_c$ (1st row, Eq. (13)), $\overline{T}$ (2nd row, Eq. (14)), $\overline{D}$ (3rd row, Eq. (15)), $\overline{P}$ (4th row, Eq. (16)) and $COT$ (5th row, Eq. (17)) as a function of $Re_f$, $Re_c$ and $DC$ for pitching (left panel) and heaving (right panel) plates. The coefficients $(\alpha,\beta,\gamma)$ are selected as $(1.5,3,3)$ and $(1.5,1,2.7)$ for pitching and heaving motions. The symbol shape square, circle and diamond are chosen to represent different amplitudes of motion from small to large, namely $\theta_0=(\pi/18,\pi/9,\pi/6)$ for pitching and $A/L=(0.1,0.3,0.5)$ for heaving, and different color red, green and blue colors represent frequencies of motion $f=(0.5,1,2)$. In addition, the orange and magenta square symbols in the subfigure (b) are data from Liu et al.[12], Dai et al.[9]. The comparison shows a good correlation between the scaling law derived in Section 2.2 and the data from the current and the previous studies

$(0,1]$, for $1 \le \beta \le 1.5$ the minimum of $COT$ is at $DC = 1$ (CS), namely CS is more efficient than IS, while for $\beta > 1.5$, compared with CS, IS can reduce energy consumption by up to $[1-(3/\beta)^{1.5}(\sqrt{\beta-1}/2)]$ at $DC_{ME}$. In other word, the energy efficiency of IS is not inherently higher than CS, and is dependent on the parameter $\beta$, which was observed in the previous study[8, 9, 31].

### 2.3 *Comparison between model-based scaling laws and numerical results*

To assess the validity of the scaling laws derived in Section 2.2, we plot the data from the current simulation as well as from the previous studies[9, 12] in Fig. 5 for $Re_c$, $\bar{T}$, $\bar{D}$, $\bar{P}$ and $COT$ as functions of $Re_f$, $Re_c$ and $DC$. Specifically, we set the $x$ axes to be the right-hand terms of Eqs. (13)-(17) for the corresponding quantities. Hence, if the result accords with the scaling law derived above, the data in Fig. 5 will fall onto the diagonal (the black dashed line) in each sub-figure. The comparison in Fig. 5 shows a good correlation between the scaling laws derived from a simplified dynamic model and the data from the current and the previous studies, except for the small deviation of $\bar{T}$ for the heaving motion in Fig. 5(d), demonstrating the viability of the current scaling law for the IS of a self-propelled plate.

Apart from the non-dimensional parameters, it is also essential to identify the coefficients in the scaling laws, and we selected $(\alpha,\beta,\gamma)$ as $(1.5,3,3)$ and $(1.5,1,2.7)$ for the pitching and heaving motions to better fit to the data.

To begin with, $\alpha$ reflects the dependence of drag on the cruising speed, and it is found that $\alpha = 1.5$ is consistent with the previous results[19] for continuous swimming in low Reynolds number flow, i.e., $Re_c \sim Re_f^{4/3}$ by letting $DC = 1$.

In addition, $\beta$ quantifies the drag difference between the burst and coast phases, as shown in Fig. 3(b). Specifically, $\beta$ is found to be 3 for the pitching, indicating that the drag coefficient of the burst phase is about three times that of the coast phase, which is consistent with the previous experiment data[6, 32]. As for the heaving, $\beta$ is 1, suggesting almost identical drag experienced by the plate during both the burst and coast phases. Similar results were observed for the heaving motion by Dai et al.[9], Liu et al.[12].

Moreover, $\gamma$ describes the scaling relationship between $Re_f$ and $\bar{P}$, which is found to be 3 for the pitching and 2.7 for the heaving in the current study. Such a value is consistent with the data in the previous studies[16, 21, 33], which falls in the range between flapping with a small amplitude, $\bar{P} \sim Re_f^2$ [15] and with a large amplitude, $\bar{P} \sim Re_f^3$ [34].

## 3. Conclusion

We numerically studied the IS dynamics of a self-propelled flexible plate over an extensive range of parameters and derived its corresponding scaling laws. Derived by a simplified IS dynamic model, the scaling laws successfully establish the relationship among key non-dimensional parameters that govern the propulsive performance and body kinematics (concluded in Eqs. (13)-(18)). The data from the current and previous studies demonstrate the validity of the derived scaling laws, which, in turn, helps to shed light on and explain several phenomena observed in the IS studies, i.e., IS may not always be energetically beneficial compared to CS, but is related to the drag performance of active bursting and coasting. While the current work can help to understand better the intrinsic principle of the intermittent locomotion of aquatic animals, we believe it will also inspire more in-depth researches on the hydrodynamics of IS, for example, the selection of the coefficients and their physical interpretation and dependence on the kinematics and material properties of the body as well as its influence on wake dynamics.

## Acknowledgements

This work was supported by the Startup Funding of New-joined PI of Westlake University (Grant Nos. 041030150118, 103110556022101), the Scientific Research Funding Project of Westlake University (Grant No. 2021WUFP017).

## Compliance with ethical standards

**Conflict of interest:** The authors declare that they have no conflict of interest. All authors declare that there are no other competing interests.

**Ethical approval:** This article does not contain any studies with human participants or animals performed by any of the authors.

**Informed consent:** Informed consent was obtained from all individual participants included in the study.

## References

[1] Ashraf I., Bradshaw H., Ha T. T. et al. Simple phalanx pattern leads to energy saving in cohesive fish schooling [J]. *Proceedings of the National Academy of Sciences of the United States of America*, 2017, 114(36): 9599-9604.

[2] Fish F. E., Fegely J. F., Xanthopoulos C. J. Burst-and-coast swimming in schooling fish (Notemigonus crysoleucas) with implications for energy economy [J]. *Comparative Biochemistry and Physiology Part A-Physiology*, 1991, 100(3): 633-637.
[3] Muller U. K., Stamhuis E. J., Videler J. J. Hydrodynamics of unsteady fish swimming and the effects of body size: Comparing the flow fields of fish larvae and adults [J]. *Journal of Experimental Biology*, 2000, 203(2): 193-206.
[4] Noda T., Fujioka K., Fukuda H. et al. The influence of body size on the intermittent locomotion of a pelagic schooling fish [J]. *Proceedings of the Royal Society B-Biological Sciences*, 2016, 283(1832): 20153019.
[5] Kramer D. L., McLaughlin R. L. The behavioral ecology of intermittent locomotion [J]. *American Zoologist*, 2001, 41(2): 137-153.
[6] Lighthill M. J. Large-amplitude elongated-body theory of fish locomotion [J]. *Proceedings of the Royal Society B-Biological Sciences*, 1971, 179(1055): 125-138.
[7] Videler J. Swimming movements, body structure and propulsion in cod (Gadus morhua) [M]. London: Academic Press, 1981.
[8] Akoz E., Moored K. W. Unsteady propulsion by an intermittent swimming gait [J]. *Journal of Fluid Mechanics*, 2018, 834: 149-172.
[9] Dai L., He G., Zhang X. et al. Intermittent locomotion of a fish-like swimmer driven by passive elastic mechanism [J]. *Bioinspiration and Biomimetics*, 2018, 13(5): 056011.
[10] Floryan D., van Buren T., Smits A. J. Forces and energetics of intermittent swimming [J]. *Acta Mechanica Sinica*, 2017, 33(4): 725-732.
[11] Kang L., Lu X. Y., Cui W. Intermittent swimming of two self-propelled flapping plates in tandem configuration [J]. *Physics of Fluids*, 2022, 34(1): 11905.
[12] Liu K., Huang H., Lu X. Y. Hydrodynamic benefits of intermittent locomotion of a self-propelled flapping plate [J]. *Physical Review E*, 2020, 102(5): 053106.
[13] Ryu J., Sung H. J. Intermittent locomotion of a self-propelled plate [J]. *Physics of Fluids*, 2019, 31(11): 111902.
[14] Gupta S., Thekkethil N., Agrawal A. et al. Body-caudal fin fish-inspired self-propulsion study on burst-and-coast and continuous swimming of a hydrofoil model [J]. *Physics of Fluids*, 2021, 33(9): 091905.
[15] Theodorsen T. General theory of aerodynamic instability and the mechanism of flutter [R]. Washington DC, USA: National Advisory Committee for Aeronautics, 1935.
[16] Quinn D. B., Moored K. W., Dewey P. A. et al. Unsteady propulsion near a solid boundary [J]. *Journal of Fluid Mechanics*, 2014, 742: 152-170.
[17] Triantafyllou G. S., Triantafyllou M. S., Grosenbaugh M. A. Optimal thrust development in oscillating foils with application to fish propulsion [J]. *Journal of Fluids and Structures*, 1993, 7(2): 205-224.
[18] Floryan D., van Buren T., Rowley C. W. et al. Scaling the propulsive performance of heaving and pitching foils [J]. *Journal of Fluid Mechanics*, 2017, 822: 386-397.
[19] Gazzola M., Argentina M., Mahadevan L. Scaling macroscopic aquatic locomotion [J]. *Nature Physics*, 2014, 10(10): 758-761.
[20] Lin X., Wu J., Zhang T. Self-directed propulsion of an unconstrained flapping swimmer at low Reynolds number: Hydrodynamic behaviour and scaling laws [J]. *Journal of Fluid Mechanics*, 2021, 907: R3.
[21] Liu K., Liu X., Huang H. Scaling the self-propulsive performance of pitching and heaving flexible plates [J]. *Journal of Fluid Mechanics*, 2022, 936: A9.
[22] Li B. L., Wang Y. W., Yin B. et al. Self-propelled swimming of a flexible filament driven by coupled plunging and pitching motions [J]. *Journal of Hydrodynamics*, 2021, 33(1): 157-169.
[23] van Buren T., Floryan D., Wei N. et al. Flow speed has little impact on propulsive characteristics of oscillating foils [J]. *Physical Review Fluids*, 2018, 3(1): 013103.
[24] Wu G., Yang Y., Zeng L. Kinematics, hydrodynamics and energetic advantages of burst-and-coast swimming of koi carps (Cyprinus carpio koi) [J]. *Journal of Experimental Biology*, 2007, 210(12): 2181-2191.
[25] Chen S., Doolen G. D. Lattice boltzmann method for fluid flows [J]. *Annual Review of Fluid Mechanics*, 1998, 30: 329-364.
[26] Doyle J. F. *Nonlinear analysis of thin-walled structures: Statics, dynamics, and stability* [M]. 1st Edition, New York, USA: Springer, 2001.
[27] Peskin C. S. The immersed boundary method [J]. *Acta Numerica*, 2002, 11: 479-517.
[28] Hua R. N., Zhu L., Lu X. Y. Locomotion of a flapping flexible plate [J]. *Physics of Fluids*, 2013, 25(12): 121901.
[29] Bottom R. G., Borazjani I., Blevins E. L. et al. Hydrodynamics of swimming in stingrays: Numerical simulations and the role of the leading-edge vortex [J]. *Journal of Fluid Mechanics*, 2016, 788: 407-443.
[30] Newbolt J. W., Zhang J., Ristroph L. Flow interactions between uncoordinated flapping swimmers give rise to group cohesion [J]. *Proceedings of the National Academy of Sciences of the United States of America*, 2019, 116(7): 2419-2424.
[31] Ashraf I., van Wassenbergh S., Verma S. Burst-and-coast swimming is not always energetically beneficial in fish (Hemigrammus bleheri) [J]. *Bioinspiration and Biomimetics*, 2021, 16(1): 016002.
[32] Webb P. W. The swimming energetics of trout: I. Thrust and power output at cruising speeds [J]. *Journal of Experimental Biology*, 1971, 55(2): 489-520.
[33] Lighthill M. J. *Mathematical biofluiddynamics* [M]. Philadelphia, USA: SIAM, 1975.
[34] Floryan D., van Buren T., Smits A. J. Efficient cruising for swimming and flying animals is dictated by fluid drag [J]. *Proceedings of the National Academy of Sciences of the United States of America*, 2018, 115(32): 8116-8118.